# Globally Optimal Transmitter Placement for Indoor Wireless Communication Systems

J. He, A. Verstak, L. T. Watson, *Fellow, IEEE*, C. A. Stinson, N. Ramakrishnan, C. A. Shaffer,

T. S. Rappaport, *Fellow, IEEE*, C. R. Anderson, *Student Member, IEEE*,

K. Bae, *Student Member, IEEE*, J. Jiang, *Student Member, IEEE*, and W. H. Tranter, *Fellow, IEEE*

***Abstract*—In this paper, a global optimization technique is applied to solve the optimal transmitter placement problem for indoor wireless systems. An efficient pattern search algorithm—DIRECT (DIviding RECTangles) of Jones, Perttunen, and Stuckman (1993)—has been connected to a parallel 3D radio propagation ray tracing modeler running on a 200-node Beowulf cluster of Linux workstations. Surrogate functions for a parallel WCDMA (wideband code division multiple access) simulator were used to estimate the system performance for the global optimization algorithm. Power coverage and BER (bit error rate) are considered as two different criteria for optimizing locations of a specified number of transmitters across the feasible region of the design space. This paper briefly describes the underlying radio propagation and WCDMA simulations and focuses on the design issues of the optimization loop.**

***Index Terms*—bit error rate, DIRECT algorithm, global optimization, power coverage, ray tracing, surrogate function, transmitter placement, wideband code division multiple access.**

## I. Introduction

Optimal transmitter placement provides high spectral efficiency and system capacity while reducing network costs, which are the key criteria for wireless network planning. As the complexity and popularity of modern wireless networks increases, automatic transmitter placement provides cost savings when compared to the traditional human process of site planning. Automatic design tools are being developed to offer efficient and optimal planning solutions. The system described here, $S^4W$ (Site-Specific System Simulator for Wireless system design), is among the few known wireless system tools for in-building network design, besides [2], [6], [8], and [12]. An optimization loop in $S^4W$ is proposed to maximize the efficiency of simulated channel models and surrogate functions are proposed to reduce the cost of simulations. Transmitter placement optimization is one specific problem that can be solved by $S^4W$. The key contributions of the present work are surrogate modeling, application of the DIRECT algorithm, and the simulation results.

J. He, A. Verstak, L. T. Watson, C. A. Stinson, N. Ramakrishnan and C. A. Shaffer are with the Department of Computer Science, Virginia Polytechnic Institute, Blacksburg, VA 24061-0106. T. S. Rappaport is with the Department of Electrical and Computer Engineering, University of Texas at Austin, Austin, Texas. C. R. Anderson, K. Bae, J. Jiang, and W. H. Tranter are with the Bradley Department of Electrical and Computer, Virginia Polytechnic Institute, Blacksburg, VA 24061-0111. This work was supported in part by NSF Grant DMI-9979711, and NSF Grant EIA-9974956.

In general, transmitter placement optimization is aimed at ensuring an acceptable level of wireless system performance within a geographical area of interest at a minimum cost. [2] considers the major performance factor to be the power coverage, defined as the ratio of the number of receiver locations with received power above an assumed threshold to the total number of receiver locations. In [6] and [10], the objective function is based on several weighted factors, such as covered area, interference area, and mean signal path loss. [1] proposes a QoS (Quality of Service)-based penalty function resulting in an unconstrained optimization problem. The present work considers two performance metrics that are continuous penalty functions defined in terms of power coverage levels and bit error rates at given receiver locations within the covered region. Both objective functions are devised to minimize the average shortfall of the estimated performance metric with respect to the corresponding threshold. 3D ray tracing is used as a deterministic propagation model to estimate power coverage levels and impulse responses within the region of interest for transmitter locations sampled by the optimization algorithm [9]. Surrogates for the Monte Carlo WCDMA simulation are used to estimate the BERs (bit error rates) for the second optimization criterion. Both the surrogates and the WCDMA simulation utilize the impulse responses estimated by the ray tracing model. Since 3D ray tracing and WCDMA simulation are computationally expensive, MPI-based parallel implementations are used in the present work.

The underlying optimization algorithm is known as DIRECT (DIviding RECTangles), a direct search algorithm proposed by Jones et al. [7]. It was proposed as an effective approach to solve global optimization problems subject to simple constraints. Jones et al. [7] named the algorithm after one of its key steps—dividing rectangles. DIRECT is a pattern search method that is characterized by a series of exploratory moves that consider the behavior of the objective function at a pattern of points, which are chosen as the centers of rectangles. This center-sampling strategy reduces the computational complexity, especially for higher dimensional problems. Moreover, DIRECT adopts a strategy of balancing local and global search by selecting potentially optimal rectangles to be further explored. This work extends that in [11], the second known application of DIRECT to wireless communication systems design.

## II. Surrogate Modeling

A simplified propagation model based on [9] is used with additional reflections incorporated. Neither diffraction nor scattering are modeled for computational complexity reasons. In addition, octree space partitioning and image parallelism with dynamic scheduling are used to reduce simulation run time. Modeling details are in [11].

This propagation model predicts a measured impulse response $P_1^m$, $P_2^m$, $\ldots$, $P_n^m$ of a wireless channel, but it does not directly predict the performance of any particular wireless system that operates in this channel. A meaningful performance metric is the bit error rate (BER) defined as the ratio of the number of incorrectly received bits to the total number of bits sent. The power level $P_1^m$ at the receiver location maps directly to the BER of a narrowband system designed for $n = 1$. However, estimating the BER of a wideband system (designed for $n > 1$) in a mobile wireless environment usually involves analytically non-tractable problems. This work uses simple least squares and multivariate adaptive regression splines (MARS [3]) to fit the results of a Monte Carlo simulation of a WCDMA system. The WCDMA simulation models channel variation due to changes in the environment as a random process and models the wireless channel as a linear time varying process. [11] contains the complete modeling details.

The WCDMA simulation is computationally intensive since a satisfactory BER value ranges from $10^{-3}$ to $10^{-6}$. The parallelized WCDMA simulator significantly speeds up the simulation process, but its run time is still far from practical for optimization problems. The BER depends on small-scale propagation effects that exhibit large variation with respect to receiver location. Practical coverage optimization problems involve wavelengths of less than a foot and areas of thousands of square feet. Four samples per wavelength should be taken to obtain meaningful aggregate results. Therefore, the BER results of the WCDMA simulation were approximated by simple models.

Consider a distribution of impulse responses in the environment , as measured by the receiver with the carrier frequency 900 HMz, the standard chip width $\delta \approx 260$ ns, and a dynamic range (a ratio of the peak power to the noise level) of 12 dB. Empirically, 49% of the impulse responses have only one multipath component ($n = 1$), 42% have two multipath components where the first one is dominant ($n = 2$, $P_1^m \geq P_2^m$), 7% have two multipath components where the second one is dominant ($n = 2$, $P_1^m < P_2^m$), and the remaining 2% have three multipath components ($n = 3$). It turns out that simple models can approximate the BERs at the majority of the receiver locations. This work considers the first two cases that account for 91% of the data.

Given a measured impulse response $P_1^m$, $P_2^m$, ..., $P_n^m$, define the relative strength of the first multipath component $p_1 = P_1^m / \sum_{1 \le i \le n} P_i^m$ and the signal-to-noise ratio (SNR) $S = \max_{1 \le i \le n}\{10 \log_{10}(P_i^m/N_0)\}$ (in dB), where $N_0$ is the noise power level (in watts).

The BER $b_1$ of a WCDMA system in the first case ($n = 1$, $p_1 = 1$) was approximated by $\log_e(b_1) = -0.251S - 2.258$, obtained by a linear least squares fit of the simulated BERs for $S = 0, 2, \ldots, 30$ in steps of 2 dB (16 points). In other words, the BER of a WCDMA system with a single path is a simple monotonically decreasing function of the SNR. This observation justifies the use of power levels to predict system performance when there is no multipath. However, using the strongest multipath component to predict the BER does not work when $n > 1$.

The second case ($n = 2$, $p_1 \ge 0.5$) was approximated using MARS models. The MARS models provided a more accurate fit to the data in comparison with the previously used linear least squares fit ([11]), reducing both the relative and absolute error. The MARS fit is a sum of products of univariate functions in the form

$$f(x) = a_0 + \sum_{n=1}^{M} a_n \prod_{k=1}^{K_n} B_{kn}\left(x_{v(k,n)}\right).$$

In this model, the multivariate spline basis functions are denoted by $B$, and their associated coefficients by $a$. This expansion of spline basis functions determines the number of basis functions, $M$, as well as product degree and knot locations (number of splits that gave rise to $B_n$ is denoted by $K_n$) automatically from the data. In this model, the covariates are represented by $x$, where $v_{(k,n)}$ label the predictor variables. MARS models were developed for three different coding choices: no channel coding, rate 1/3 coding, and rate 1/2 coding. The latter two cases both use FECC (forward error correction code) to improve the BER performance. A soft decision Viterbi algorithm is used in decoding the convolutional FECC, because it produces a smaller BER than the hard decision Viterbi algorithm. The difference between these two cases lies in the convolutional code rate. Rate 1/3 coding provides a better error correction mechanism than the rate 1/2 coding.

The data used to build the no channel coding model consisted of 63 points from a Cartesian product of $S = 0, 1, \ldots, 20$ and $p_1 = 0.9, 0.7, 0.5$, and 48 points from a Cartesian product of $S = 0, 1, \ldots, 15$ and $p_1 = 0.9, 0.7, 0.5$ for the channel coding models. Plots of the fitted models reveal that the BER approaches zero as the SNR increases and that stronger multipath significantly improves performance for a fixed SNR. The latter needs some explanation because multipath is often thought of as an impairment that degrades the system performance. In this work, the SNR is defined in terms of the strongest component of the impulse response. When the SNRs of two channels that meet the criteria for this case are the same, the channel with a stronger second component contains more total power than the channel with a weaker second component. In this case, the benefits of more power outweigh the disadvantages of multipath.

Both surrogate models were validated with the simulated BER results. In the first case, the approximate values had an average relative error of 9.7% (0.9% minimum, 19.4% maximum) for the simulation output at $S = 1, 3, \ldots, 29$. In the second case, the approximate values had an average relative error of 12.8% and average absolute error of 0.0006 for the no channel coding model, 14.1% average relative error and 0.0005 average absolute error for the rate 1/3 coding model, and 19.9% average relative error and 0.0012 average absolute error for the rate 1/2 coding model. The validation sets for the second case consisted of 42 points for a Cartesian product of $S = 1, 2, \ldots, 20$ and $p_1 = 0.8, 0.6$ for the no channel coding model, and 32 points for a Cartesian product of $S = 1, 2, \ldots, 15$ and $p_1 = 0.8, 0.6$ for the channel coding models.

Finally, observe that the models for the two cases are not asymptotically matched. The simulated WCDMA receiver had two rake fingers, one of which was turned on or off depending on whether or not the second multipath component met the relative power threshold. Empirically, both models cover 91% of the data with about 9.7% average relative error for the least squares model and 15.6% average relative error and 0.0008 average absolute error for the MARS models. The quality of the MARS approximation is apparent in Figure 2.1, which shows the MARS spline surface for the no channel coding model, the points used to construct it ($p_1 = 0.9, 0.7, 0.5$), and the points used to validate the approximation ($p_1 = 0.8, 0.6$).

## III. DIRECT

Starting from the center of the initial design space $\{x \in E^n \mid \ell \leq x \leq u\}$ normalized to a unit hypercube, DIRECT makes exploratory moves across the design space by probing and subdividing potentially optimal subsets, which are most likely to contain the global minimum. "Potentially optimal" has a precise mathematical definition [7] based on a Lipschitz condition. The DIRECT box selection strategy prevents the search from becoming too local, and ensures that a nontrivial improvement will (potentially) be found based on the current best solution.

Choices for a stopping condition include an iteration limit, a function evaluation limit, minimum diameter (terminate when the best potentially optimal box's diameter is less than this minimum diameter), and objective function convergence tolerance (exit when the objective function does not decrease sufficiently between iterations). The objective function convergence tolerance was inspired by some experimental observations running the DIRECT algorithm, where the objective function sharply decreases at the beginning and levels off at the end (see Figure 4.3 of Section IV). The objective function convergence tolerance is defined as $\tau_f = (\tilde{f}_{\min} - f_{\min})/(1.0 + \tilde{f}_{\min})$, where $\tilde{f}_{\min}$ represents the previous computed minimum. The algorithm stops when $\tau_f$ becomes less than a user specified value.

The present implementation of the DIRECT algorithm addresses an efficiency issue involved in an unpredictable storage requirement in the phase of space partitioning. The main problem to be solved is how to store the large collection of boxes, typically viewed as a set of separate columns. The key operations are to find the element in a column with least value, to remove this least-valued element, and to add new elements to a column. Thus each column can be viewed abstractly as a priority queue. Implementation details are given in [5].

As [7] proved, the DIRECT algorithm is guaranteed to converge globally if the objective function is Lipschitz continuous. However, the original definitions for both performance criteria—power coverage and BER (bit error rate) do not satisfy this condition. Similar to the power coverage criterion introduced in Section I, BER is the ratio of bits that have errors relative to the total number of bits received in a transmission. Reformulation is required to eliminate the discontinuity.

Transmitters are assumed to operate at sufficiently different frequencies so that receivers can pick up the strongest signal. In other words, the indoor environment is only considered as a coverage-limited one, which is different from an interference-limited environment, where the outage is a result of cochannel signals dominating or interfering with the wanted signals [1]. Such an environment presents more complexities and challenges for implementing the WCDMA channel model. In the present work, the ray tracing technique serves as a deterministic way to calculate the local mean signal power propagating from the transmitter to each receiver on the reception grid.

As in [2], the design variables are the transmitter coordinates $X = (x_1,\ y_1,\ z_1,\ x_2,\ y_2,\ z_2,\ \ldots,\ x_n,\ y_n,\ z_n)$, where all $z_j = z_0$ are assumed to be fixed, which is a reasonable assumption in indoor environments. Permuted coordinates will occur during optimization, since the DIRECT algorithm treats the function as a black box and has no knowledge of any symmetry relationships. A solution is to simply sort coordinates on each dimension, and buffer current pairs of sorted coordinates and the corresponding function values. When the permuted coordinates are detected by the optimizer, the function value will be taken directly from the buffer instead of calling the ray tracer to reevaluate the function.

With the stated assumption and the design variables above, the single transmitter location problem is a special case of the $n$ transmitter problem with $n = 1$. The goal is to minimize the average shortfall (power coverage or bit error rate) of the $n$ transmitters over $m$ receiver locations. Let transmitter $(k, i)$, located at $(x_k, y_k, z_0)$, $1 \le k \le n$, generate the highest peak power level $P_{ki}(x_k, y_k, z_0) \ge P_{ji}(x_j, y_j, z_0)$, $1 \le j \le n$, at the receiver location $i$, $1 \le i \le m$. The objective function is the average shortfall of the estimated performance metric from the given threshold $T$, given by

$$f(X) = \begin{cases} \dfrac{1}{m}\displaystyle\sum_{i=1}^{m}(T - p_{ki})_+, & \text{coverage,} \\ \dfrac{1}{m}\displaystyle\sum_{i=1}^{m}(p_{ki} - T)_+, & \text{BER,} \end{cases}$$

where $p_{ki}$ is the performance metric of transmitter $(k, i)$ evaluated at the $i$th receiver location. For power coverage optimization, $p_{ki}$ is $P_{ki}(x_k, y_k, z_0)$ and $(T - p_{ki})_+$ is the penalty for a low power level. For BER optimization, $p_{ki}$ is $\mathrm{BER}_{ki}$ and $(p_{ki} - T)_+$ is the penalty for a high bit error rate.

## IV. Optimization Results

Optimization was done using a problem solving environment (PSE) as outlined in [11]. Transmitter placement was optimized executed for two indoor environments with respect to the two performance criteria—power coverage and BER. The first environment, located on the fourth floor of Durham Hall at Virginia Tech, was the first case study for the global optimization technique. Simulations have been verified with measurement data on the first environment [11]. The second environment had been used in both raytracing simulations and measurements in [9], which considers signal diffractions in the propagation model so that it can match well the measured and predicted propagation in a variety of indoor environments. (The propagation model code of [9], while having better physics than the present ray tracing code, is orders of magnitude slower because of inefficient data structures.) Table 4.1 summarizes the simulation results, discussed in detail in [4], on both environments.

*A. Durham Hall, fourth floor.* The results of optimizing the transmitter placement in the case of power coverage are shown in Figure 4.1. For a single transmitter, it took 41 evaluations (3 minutes, 45 seconds) to reduce the objective function by 22.2% (from 4.60 dB to 3.58 dB). For optimizing three transmitter locations to cover the region of interest in the upper-left corner, it took 93 function evaluations to reduce the objective by 9.4% (from 2.77 dB to 2.51 dB) in 38 minutes on 40 machines. Figure 4.2 depicts BER optimization of the locations of two transmitters to cover half of the former region. In Figure 4.2 (a), 56 iterations reduced the objective function from 8.24e-4 to 1.65e-4 in 3 hours and 26 minutes on 40 machines. The BER threshold was $10^{-3}$, so this improvement corresponds to a 79.9% reduction in the average BER. Figure 4.2 (b) shows that the percentage of the receivers with satisfied BER is growing as the objective function decreases. In both cases, the optimization loop stops with the minimum diameter required by the problem. System performance was significantly improved by DIRECT with a reasonable number of evaluations.

Figure 4.3 demonstrates the effectiveness of the new stopping criterion—objective function convergence tolerance. This figure shows the power coverage optimization results for two transmitters. Two simulations were done with different objective function convergence tolerances—0 and 0.001. In the former case, it took 52 iterations to reach the final locations (marked as crosses). In the latter case, the final locations (marked as triangles) were found after 27 iterations. Using a nonzero objective function convergence tolerance saved 25 expensive ray tracing iterations.

*B. Whittemore Hall, second floor.* Figure 4.4 shows the results for optimizing the placement for a single transmitter and three transmitters in terms of both power coverage and BER. To optimize the single transmitter location, the minimum diameter stopping criterion was used. It took 6 more evaluations for the BER optimization to finish than the power coverage optimization. Since BER simulation is affected by numerous system and channel parameters such as signal-to-noise ratio, data rate, modulation type, etc., it is very sensitive to parameter changes caused by changing transmitter locations. The objective function for BER exhibits more complexity (both multipath components are involved when there are two resolvable paths) than the one for power coverage (only the dominant multipath component is considered), therefore it takes more evaluations to approach the global optimum. Figure 4.4 (left) shows that the final locations are different (cross for powers, triangle for BER). Generally, BER optimization results are preferred, since BER is considered a better performance criterion in the design of mobile communication systems as pointed out in Section II. In the case of optimizing three transmitter locations, the stopping criterion was the maximum number of evaluations. Both BER and coverage optimization stopped at the 54th iteration. The exact same final transmitter locations were reached at the 51st iteration. Interestingly, the final locations are exactly the same (marked as crosses at the top of Figure 4.4 on the right). This indicates a reasonable connection between these two performance metrics—power coverage and BER.

The cost and improvement for these four experiments on the second floor of Whittemore Hall are compared in Table 4.1. In both cases, the BER optimization achieved a better improvement than the power coverage optimization with almost the same cost. For the single transmitter, the objective function value of the BER optimization was reduced by 60.7% while the power coverage optimization improved only by 37.7%. In the case of three transmitters, the objective function was reduced by 48.9% for the power coverage optimization and by 64.2% for the BER optimization. From this comparison, the DIRECT algorithm works very cost-effectively for BER optimization problems. On the other hand, the center-sampling strategy of DIRECT benefits the power coverage optimizations by starting at the centers of bounded areas, so that the well-distributed initial locations only need a little adjustment. This can also explain why the power coverage optimization gave less improvement.

## V. Conclusion

The main contribution of the present work is the design of an optimization loop that takes feedback from a sophisticated surrogate model of a wireless system. The DIRECT algorithm effectively solved the global optimization problem of transmitter placement. Extensions to the present work include BER surrogate functions for channels with relatively strong multipath and interference, and consideration of wireless systems with data quality bit error rates ($10^{-6}$).

## References


[1] K. W. Cheung and R. D. Murch, "Optimizing indoor base station locations in coverage- and interference-limited indoor environments," in *IEE Proceedings-Communications*, vol. 143(6), pp. 445–450, 1998.

[2] S. J. Fortune, D. M. Gay, B. W. Kernighan, O. Landron, R. A. Valenzuela, and M. H. Wright, "WISE design of indoor wireless systems: practical computation and optimization," *IEEE Computational Science & Engineering*, vol. 2(1), pp. 58–68, Spring, 1995.

[3] J. H. Friedman, "Multivariate adaptive regression splines," *Annals of Statistics*, vol. 19(1), pp. 1–67, 1991.

[4] J. He, A. Verstak, L. T. Watson, C. A. Stinson, N. Ramakrishnan, C. A. Shaffer, T. S. Rappaport, C. R. Anderson, K. Bae, J. Jiang, and W. H. Tranter, "$S^4W$: globally optimized design of wireless communication systems," *Computer Science Technical Report TR-02-16, Virginia Polytechnic Institute and State University*, 2002.

[5] J. He, L. T. Watson, N. Ramakrishnan, C. A. Shaffer, A. Verstak, J. Jiang, K. Bae, and W. H. Tranter, "Dynamic data structures for a direct search algorithm," *Computational Optimization and Applications*, vol. 23, pp. 5–25, 2002.

[6] X. Huang, U. Behr, and W. Wiesbeck, "Automatic base station placement and dimensioning for mobile network planning," in *Proc. of Vehicular Technology Conference*, IEEE VTS Fall VTC 2000. 52nd, vol. 4, pp. 1544–1549, 2000.

[7] D. R. Jones, C. D. Perttunen, and B. E. Stuckman, "Lipschitzian optimization without the Lipschitz constant," *Journal of Optimization Theory and Applications*, vol. 79(1), pp. 157–181, 1993.

[8] T. S. Rappaport and R. R. Skidmore, Wireless Valley Communications, Inc., *Method and System for Automated Optimization of Antenna Positioning in 3-D*, US Patent 6,317,599, November, 2001.

[9] S. Y. Seidel and T. S. Rappaport, "Site-specific propagation prediction for wireless in-building personal communication system design," *IEEE Transactions on Vehicular Technology*, vol. 43(4), pp. 879–891, 1994.

[10] H. D. Sherali, C. M. Pendynala, and T. S. Rappaport, "Optimal location of transmitters for micro-cellular radio communication system design," *IEEE Journal on Selected Areas in Communications*, vol. 14(4), pp. 662–673, 1996.

[11] A. Verstak, J. He, L. T. Watson, N. Ramakrishnan, C. A. Shaffer, T. S. Rappaport, C. R. Anderson, K. Bae, J. Jiang, and W. H. Tranter, "$S^4W$: globally optimized design of wireless communication systems," in *16th Internat. Parallel & Distributed Processing Symp.*, CD-ROM, IEEE Computer Soc., Los Alamitos, CA, 8 pages, 2002.

[12] J. K. L. Wong, M. J. Neve, and K. W. Sowerby, "Wireless personal communications system planning using combinatorial optimisation," in *Proc. Virginia Tech's Tenth Symposium on Wireless Personal Communications*, Blacksburg, VA, June 14–16, 2000.

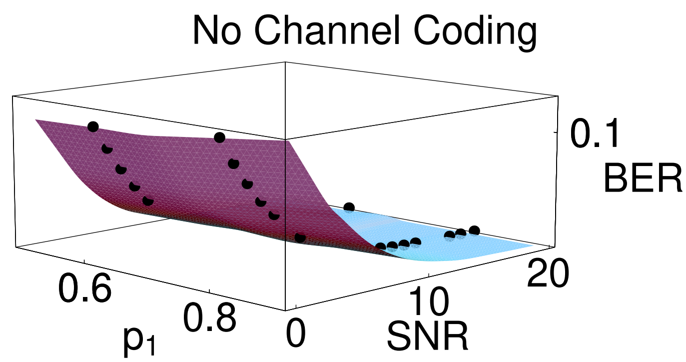


Fig. 2.1. The MARS surface plot of no channel coding model.

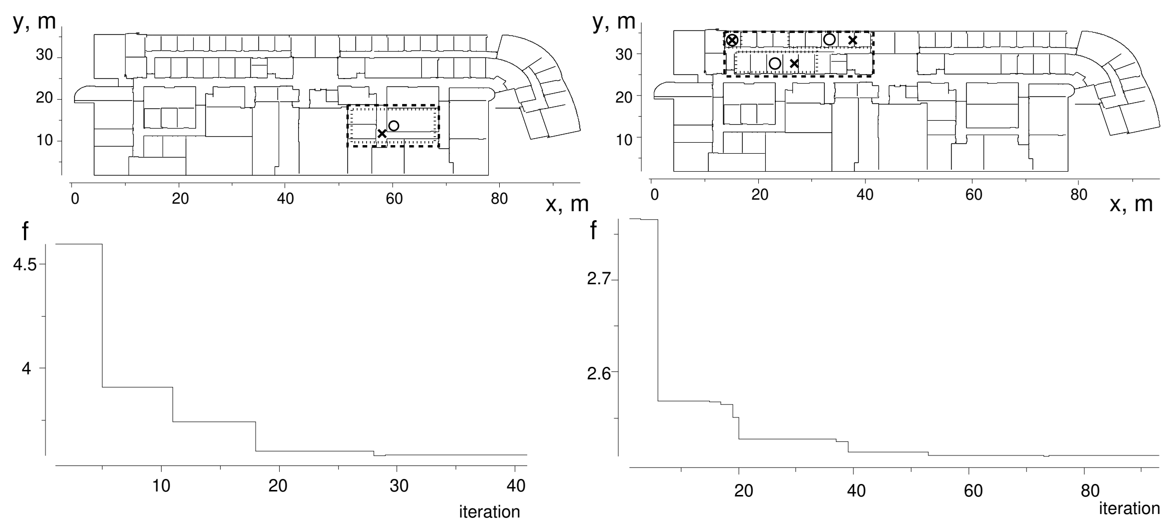


Fig. 4.1. Power coverage optimization results for a single transmitter (left) and three transmitters (right). Bounds on transmitter placement are drawn with dotted lines and their initial (final) positions are marked with circles (crosses). The dashed line delimits the region to be covered.

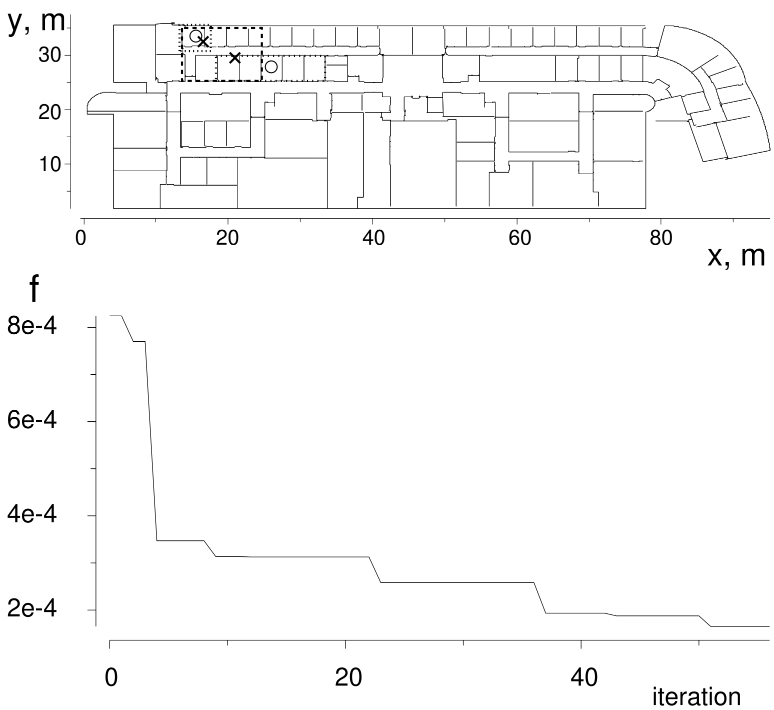


(a) Objective function.

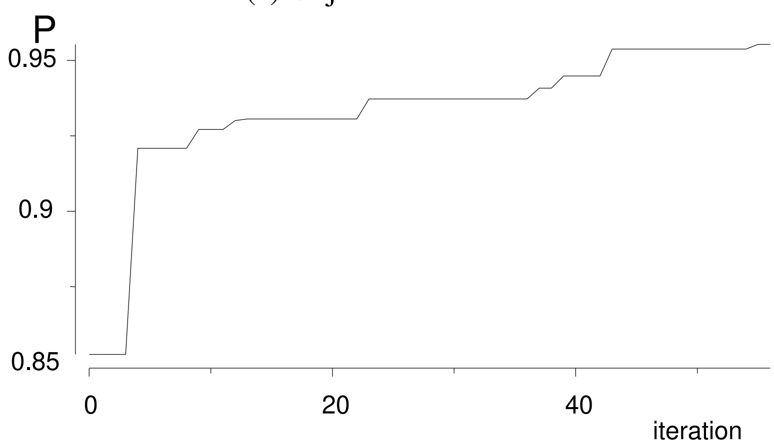


(b) Percentage of receivers with satisfied BER values.

Fig. 4.2. BER optimization results for two transmitters. Bounds on transmitter placement are drawn with dotted lines and their initial (final) positions are marked with circles (crosses). The dashed line delimits the region to be covered.

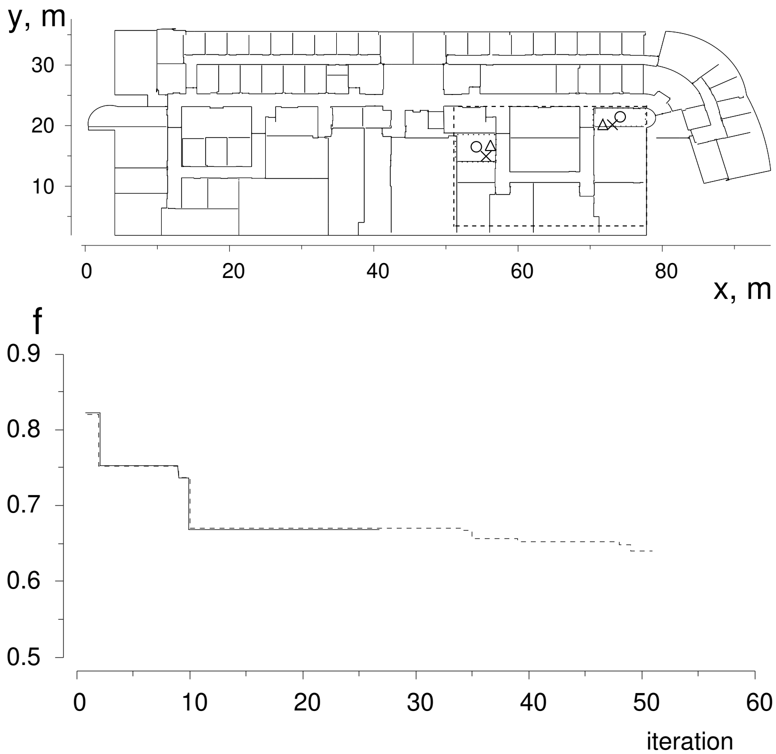


Fig. 4.3. Power coverage optimization results for two transmitters with objective function convergence tolerance = 0 (dashed) and 0.001 (solid). The region of interest is delimited by dashed lines. The initial locations are marked as circles. Bounds on transmitter placement are drawn with dotted lines.

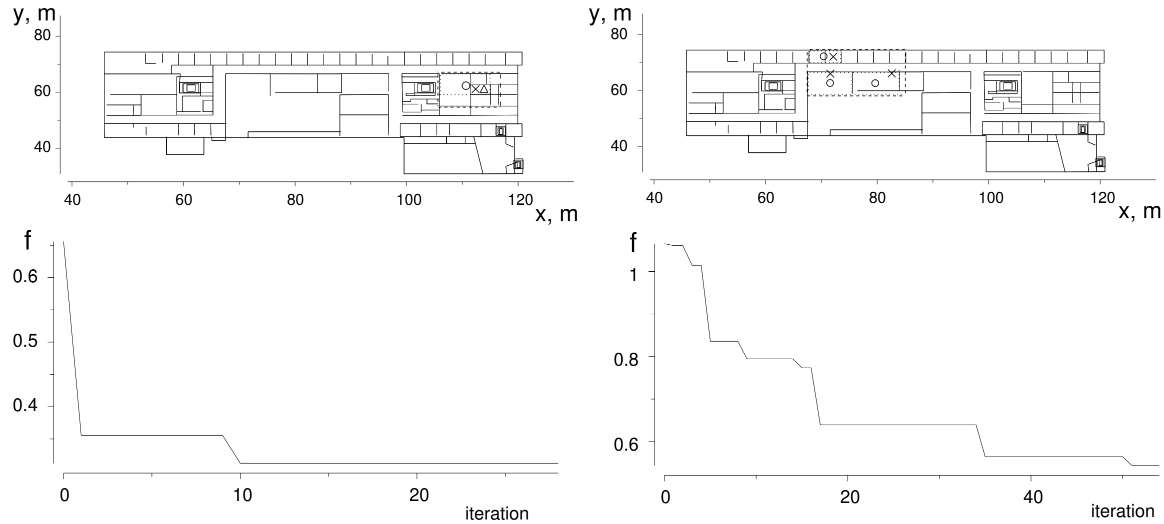


(a) Power coverage

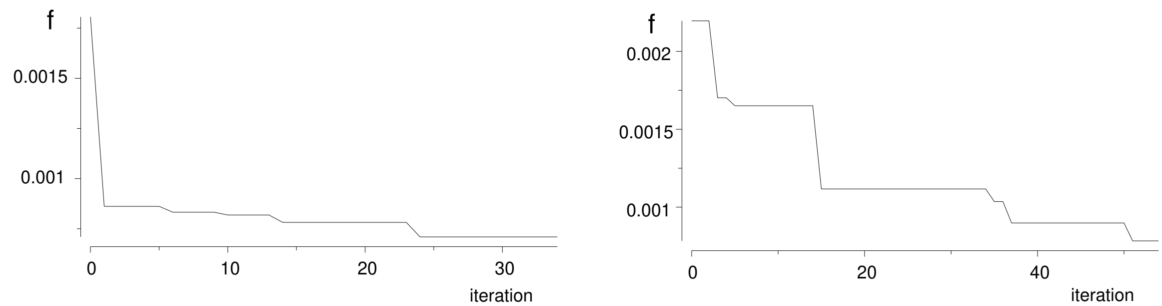


(b) BER

Fig. 4.4. Power coverage and BER optimization results for a single transmitter (left) and three transmitters (right). Bounds on transmitter placement are drawn with dotted lines and their initial (final) positions are marked with circles (crosses). The dashed line delimits the region to be covered.

Table 4.1. Summary of time, cost (number of ray tracing iterations) and improvement (relative function value reduction) for power coverage and BER optimization experiments with $N$ transmitters on Durham Hall, fourth floor and Whittemore Hall, second floor.

| | | Durham Hall | | | Whittemore Hall | |
|---|---|---|---|---|---|---|
| Objective | $N$ | time | cost | improvement | cost | improvement |
| Power | 1 | 3min, 45sec | 41 | 22.2% | 28 | 37.7% |
| BER | 1 | — | — | — | 34 | 60.7% |
| BER | 2 | 3hr, 26min | 56 | 79.9% | — | — |
| Power | 3 | 38min | 93 | 9.4% | 54 | 48.9% |
| BER | 3 | — | — | — | 54 | 64.2% |